Electron-beam-induced structural variations of divanadium pentoxide (V_2O_5) at liquid helium temperature

M. Wieske, D.S. Su *, F. Beckmann, and R. Schlögl

Department of Inorganic Chemistry, Fritz-Haber-Institute of the Max-Planck-Society, Faradayweg 4-6, D-14195 Berlin, Germany

Received 15 December 2001; accepted 3 January 2002

The electron-beam-induced changes in V_2O_5 crystals were investigated by means of electron microscopy at liquid helium temperature (4.2 K). We obtained high-resolution images of this system, but observed an amorphization process during a prolonged exposure to the electron beam. The average oxidation state of the amorphous phase was estimated to be about 4+. This phase was stable at room temperature, but a partial recrystallization occurs by further irradiation at room temperature and it can be reduced to VO. These observations are discussed with respect to the reduced diffusion rate of oxygen and lattice collapses at this very low temperature.

KEY WORDS: electron irradiation; reduction; amorphization; diffusion; V_2O_5.

1. Introduction

Vanadium oxides are the main constituents of VPO catalysts. These catalysts are widely used in a variety of chemical reactions, *e.g.* selective oxidation processes [1] or selective reduction of NO_x [2], and many efforts have already been made in the evaluation of the physical and chemical properties of vanadium oxides. Especially, phase transitions and the reduction of vanadium oxides have been studied extensively since they are the underlying phenomena that may play a key role in understanding the catalytic mechanism and developing high-performance catalysts [3–5]. Experimentally, a V_2O_5–V_6O_{13} transformation has been reported on the (001) surface by heating V_2O_5 at 500 °C under an O_2 atmosphere (5×10^{-4} Torr, 1 h) [3]. Bulk phase transition was studied by means of thermal decomposition of a mixture of V_2O_3 and V_2O_5 heated at 600 °C in vacuum, revealing a coexistence of V_2O_5, V_6O_{13}, VO_2 and V_3O_7 phases after eight days [4]. Theoretically, the V_2O_5–V_6O_{13} transformation is explained as an ordering of oxygen vacancies: if every third oxygen layer in the V_2O_5 structure is removed, shearing occurs from corner-linked to edge-linked octahedra [5].

In a previous work V_2O_5 was found to be reduced, *via* an unknown intermediate phase, to VO (a rock salt structure) under the electron beam at room temperature [6]. The reduction of V^{5+} to V^{2+} is much greater than the reduction processes described above. The reduction mechanism is unclear and cannot be explained by the crystallographic shear mechanism. In a controlled heating study in the high vacuum of the electron microscope without the effect of beam irradiation, a different reduction pathway, *i.e.* a $V_2O_5 \longrightarrow VO_2 \longrightarrow V_2O_3$ phase transformation, was observed [7]. The obtained V^{5+} to V^{3+} reduction was not as great as that induced by the electron beam, but is still greater than that through thermal decomposition mentioned above. These two reduction pathways and their discrepancy from that reported in refs. [3,4] may imply that the reduction of V_2O_5 is strongly dependent on environment and driving forces. In the present work, we focused on the phase transition and reduction of single-phase V_2O_5 crystals by electron irradiation at 4.2 K using a modified Philips CM20 electron microscope SOPHIE [8]. This is an experiment minimizing temperature-dependent effects. The structural changes were analyzed by means of electron diffraction and high resolution imaging, while changes in chemical compositions and in electronic structures (reduction state of V ions) were obtained by analyzing the electron energy-loss near-edge structure (ELNES) at room temperature.

V_2O_5 crystallizes in the orthorhombic space group *Pmmn* [1] with lattice parameters $a = 1151.2$ pm, $b = 356.4$ pm and $c = 436.8$ pm. It can be thought of as built from edge-sharing and corner-sharing VO_6 distorted octahedra in two levels, connected along *a* and *b* by a common edge so as to form zig-zag rows which are stacked along *c*. Crystalline V_2O_5 exhibits a layered structure, which can easily be cleaved along the (001) plane due to the weak bonding along the *c* axes [3].

2. Experimental

Single-phase V_2O_5 crystals were grown by a chemical vapor transport technique in a temperature-controlled two-zone furnace as described previously [6,9]. For

* To whom correspondence should be addressed.

1011-372X/02/0700-0043/0

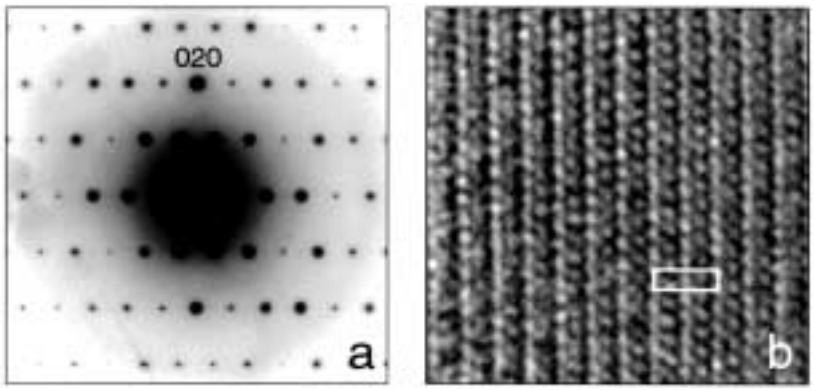

Figure 1. Electron diffraction pattern (a) and a high-resolution image (b) of a thin V_2O_5 crystal at 4.2 K. A projection of the unit cell ($a = 1151.2$ pm, $b = 356.4$ pm) is inserted in (b).

electron microscopic investigations, the V_2O_5 crystals were crushed gently in carbon tetrachloride. A drop of the solution containing fine flakes was placed on a marked 400-mesh copper grid covered with holey carbon film and allowed to dry. Due to the weak bonded structure between the layers, most of the crushed pieces were cleaved in the (001) plane and also settled down on the grid in this orientation. All investigations were performed on flakes lying over holes in the carbon film.

The cryo-electron microscope SOPHIE was used to study the structural changes at very low temperatures. This is a modified Philips CM20 FEG electron microscope with a helium-cooled superconductive objective lens [8] in which specimens are kept at a temperature of 4.2 K. Before use, the grids were plunged into liquid nitrogen and transferred into the microscope, which was operated at 200 kV. The electron dose rate was $396\,e^-/Å^2\,sec^{-1}$, the thickness of the sample was estimated to be about 20 nm and the overall irradiated area was about 700 nm in diameter. A Philips CM200 FEG electron microscope, operating at 200 kV and equipped with a GIF100 Gatan imaging filter for recording electron energy-loss spectra (EELS), was used to study the subsequent structural changes at room temperature. The electron dose rate was approximately $2000\,e^-/Å^2\,sec^{-1}$.

3. Results

3.1. V_2O_5 structure at 4.2 K

In figure 1(a), a typical diffraction pattern obtained from a fine flake is shown. The diffraction pattern is identified as the (001) pattern of V_2O_5 in the orthorhombic structure with the space group *Pmmn* [10], indicating that there is no structural transformation of V_2O_5 at this very low temperature. After switching to imaging mode we obtained high-resolution images representing the well-ordered structure of the V_2O_5 crystals in (001) orientation. The Fourier transformation of the high-resolution image reveals the good match to the orthorhombic structure of (001) oriented vanadium pentoxide. (200) lattice fringes run in a vertical direction with a spacing of 0.57 nm. A sketch of the (001) projection of the V_2O_5 unit cell is inserted in figure 1(b).

3.2. Structural changes induced during irradiation at 4.2 K

In figure 2, a series of high-resolution images is depicted showing representative steps of the alterations occurring during irradiation of a V_2O_5 crystal at 4.2 K in the SOPHIE microscope. The appearance of the initial state (figure 2(a)) is comparable with the high-resolution

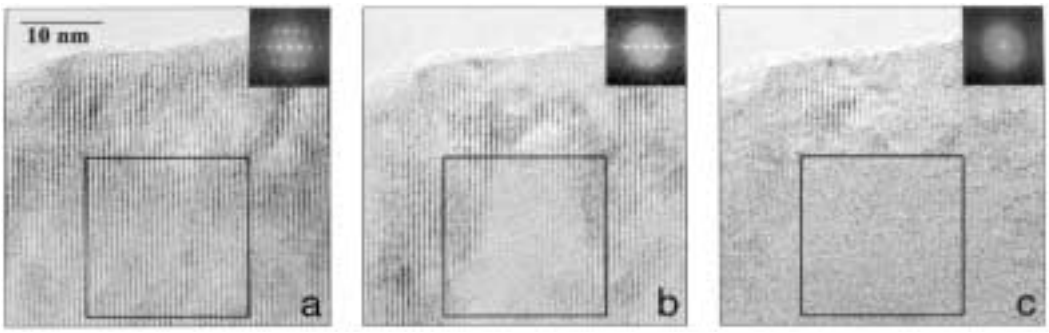

Figure 2. HREM imaging series indicating the structural changes during electron exposure at 4.2 K. Insets show corresponding power spectra calculated from the outlined area. Images a, b and c were taken after electron doses of 38, 457 and 723 A sec/cm^2, respectively. The bar represents 10 nm.

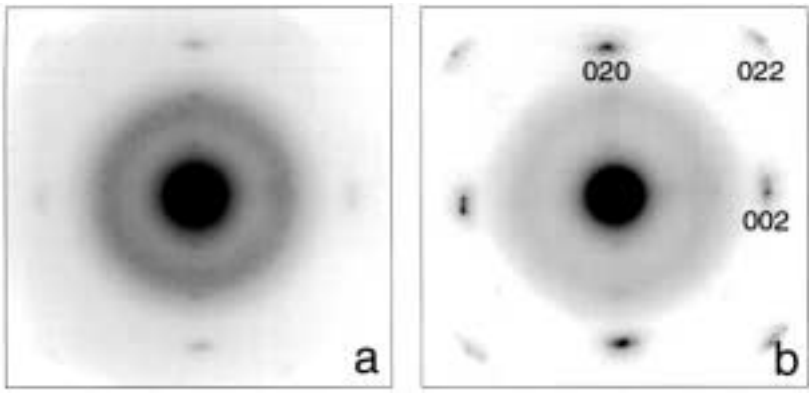

Figure 3. Illustration of the structural changes of V_2O_5 (001) by electron irradiation at different temperatures: (a) amorphous sample, irradiated extensively at 4.2 K, transferred to the CM200 FEG microscope and observed at room temperature; (b) the same sample after prolonged exposure to the electron beam at room temperature. Indices due to VO in rock salt structure are inserted.

image shown in figure 1(b). The (200) as well as some other lattice fringes are recognizable. After moderate illumination under the electron beam (457 A sec/cm^2, figure 2(b)), an amorphous region in the middle of the depicted area appears, which starts to spread out over a wider region. After an electron dose of 723 A sec/cm^2, most of the observed area has become amorphous (figure 2(c)). This process can be well followed by the calculated power spectra of the marked image areas in figure 2 (inset also in figure 2). Due to the amorphization, a significant fraction of the diffracted intensity in the power spectrum (figure 2(b)) has disappeared, while the power spectrum in figure 2(c) contains only diffuse rings, confirming the amorphous character of this area. Diffuse rings were also observed in diffraction mode after prolonged irradiation. As observed in imaging mode, the amorphous sites appear randomly all over the illuminated area, which results in a patchy appearance of the specimen until the whole area becomes amorphous. During this process no defined structural changes could be recognized since the power spectra and diffraction patterns contained no additional Bragg spots.

3.3. Recrystallization at room temperature

The specimen was then transferred with an extensive irradiated (*i.e.* amorphous) area from the SOPHIE microscope to the CM200 FEG microscope and the same region was analyzed again at room temperature. It was found that the amorphous phase formed at 4.2 K was quite stable at room temperature and even at atmospheric pressure during the transport between the microscopes, as deduced from diffraction analysis: a selected area diffraction pattern from the amorphous region is reproduced in figure 3(a), showing diffuse rings. The weak spots in this pattern could be due to the re-exposure of the sample to the electron beam without cooling, which becomes clearly visible with prolonged irradiation time. An electron diffraction pattern after 20 min irradiation is shown in figure 3(b). It is evident that the beam irradiation at this temperature can induce rearrangement of atoms, partly forming long-range order again. It cannot lead to a complete recrystallization because diffuse rings in the diffraction pattern do not disappear totally even with further prolonged irradiation. The Bragg spots in figure 3(b) can be identified as those of VO in rock salt structure with lattice spacings of 0.144 and 0.205 nm.

3.4. EELS

In order to figure out the electronic structure of the amorphous phase obtained after prolonged irradiation at 4.2 K, EEL spectra from the irradiated area and standard samples were recorded. Figure 4 shows spectra after background and multiple scattering corrections [11]. Spectra a and d are reference spectra from V_2O_5 and VO, respectively. Spectrum b was recorded on the

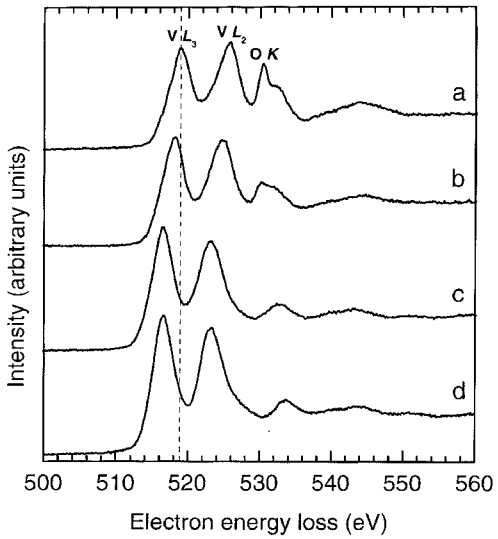

Figure 4. V L and O K ELNES from samples of fresh V_2O_5 (a), V_2O_5 after extensive irradiation at 4.2 K (b), V_2O_5 after further irradiation at room temperature (c) and, for comparison, of fresh VO (d).

area after extensive irradiation at 4.2 K. Spectrum c was recorded on the same area, but after further irradiation at room temperature. The main features in the spectra are vanadium $L_{2,3}$ edges at 519 and 526.5 eV, stemming from the transitions from the V $2p_{3/2,1/2}$ core levels to the unoccupied V 3*d* bands, and the oxygen *K* edge at 530 eV, stemming from the transitions from the O 1*s* core level to the unoccupied V 3*d* bands due to orbital hybridization.

Comparing spectrum b with spectrum a, a visible decrease of the integrated intensity of the oxygen *K* edge can be recognized. The loss of this intensity mirrors the change of the stoichiometric ratio of O/V in the amorphous phase: a preferential loss of oxygen took place and therefore a reduction of vanadium. Reducing the vanadium has the consequence that vanadium $L_{2,3}$ edges should shift to lower energy. In fact, the L_3 peak of vanadium in spectrum b of figure 4 is measured to be at 518.4 eV. According to a correlation between oxidation states and L_3 peak position of binary vanadium oxides, a peak position at this value corresponds to an averaged oxidation state of V^{4+} [12].

Spectrum c in figure 4 reveals that electron beam irradiation at room temperature not only induces a partial recrystallization of the studied area, but also induces the reduction of the samples through the loss of oxygen: the integrated intensity of the oxygen *K* edge decreases and the vanadium L_3 edge shifts to about 516.5 eV corresponding to the peak position of the L_3 edge of VO.

4. Discussion

We observed, by means of electron diffraction and high-resolution imaging, an electron-irradiation-induced structural change of V_2O_5 at liquid helium temperature from the highly ordered crystal *via* a patchy appearance to an amorphous state. This observation differs from other investigations of phase transitions of V_2O_5. At room temperature under a 200 kV electron beam, V_2O_5 is transformed, *via* an unknown intermediate phase, into VO in cubic rock salt structure [6]. Heating V_2O_5 in a specimen chamber of a Philips CM200 FEG electron microscope led to a $V_2O_5 \rightarrow VO_2 \rightarrow V_2O_3$ transformation [7]. In the present work, V_2O_5 is transformed to an amorphous phase with an averaged oxidation state of vanadium at V^{4+}. This oxidation state is higher than that obtained in previous works [6] and [7], where the final oxidation states of vanadium are V^{2+} and V^{3+}, respectively.

This *soft* reduction of V_2O_5 under the electron beam with the same primary energy (200 kV) as that used in ref. [6] could be explained by the very slow diffusion rate of oxygen atoms in the sample at nearly 4.2 K. At the surface and the near-surface regions oxygen atoms can still be removed by knock-on sputtering processes from the sample, forming a deficiency of the oxygen concentration at the surface. However, due to the very low sample temperature, the diffusion of bulk oxygen to the surface is inhibited so that the amount of oxygen vacancies in bulk that is required for the transformation to VO or V_2O_3 cannot be reached. Furthermore, as the electron beam breaks up the atomic bonds and the structure becomes amorphous, all the lattice channels that may facilitate the diffusion of oxygen could be destroyed or plugged.

Our observation supports on one hand indirectly the proposed reduction mechanism of V_2O_5 by the out-diffusion of oxygen out of the bulk and the subsequent formation of oxygen vacancies in bulk [5]. On the other hand, however, the crystallographic shearing mechanism, which is well accepted as an explanation of the reduction of vanadium oxide [5] and vanadium phosphorus oxides [13], cannot be applied to interpret the observed reduction since the sample becomes amorphous. In such a shear process, the sample remains crystalline, while only the lattice symmetry changes. It is obvious that the energy needed for crystallographic shearing in a *frozen* lattice is much higher than in a lattice at room or even higher temperature.

Another surprising finding of the present work is that the *frozen* amorphous state is stable at room temperature. The thermal energies at room temperature are obviously too low to induce any structural change. The further reduction under the electron beam is accompanied by a partial recrystallization. The diffusion rate of oxygen increased through electron beam irradiation *and* through the rearrangement of vanadium and oxygen atoms, which can in turn further favor the atomic diffusion in the sample. Since the interaction of the incident electron beam with the sample is independent of the sample temperature, the role of electron beam irradiation in the 4.2 K experiment is as usually found in normal experiments. Therefore we believe that the main effect of the electron bombardment is knock-out of atoms from their regular sites leading to a kind of local disordering. The rearrangement of atoms is probably impossible at this temperature. In a common TEM this disordering process cannot be observed since the atoms can begin immediately to rearrange, forming a state which is more resistant to electron beam damage. This short amorphization/rearrangement process could be the explanation for the reduction of orthorhombic V_2O_5 to cubic VO [6], a process that cannot be explained by the crystallographic shear mechanism. However, it should be mentioned that the rearrangement of atoms under the electron beam follows topotactically: at room temperature, the 001-oriented V_2O_5 was reduced to the 001-oriented VO. In the present work, although the 001-oriented V_2O_5 was first changed to a reduced amorphous phase, this phase recrystallizes and reduces also to the 001-oriented VO (compare diffraction patterns in figures 1(a) and 3(b)). The details of this *solid state epitaxy re-growth* are still unknown.

5. Summary

We analyzed the structural and reductive alterations of V_2O_5 due to electron irradiation at liquid helium temperature. An amorphization of the irradiated area occurred with increasing electron exposure. The amorphous phase was stable at room temperature and the averaged oxidation state was about 4+. Once this phase was irradiated at room temperature a partial recrystallization and reduction to VO occurred. An inhibited diffusion and a high threshold energy for atomic rearrangement, compared with that at room temperature, are held responsible for these observed changes.

Acknowledgments

The work is partly supported by SFB 546 of the Deutsche Forschungsgemeinschaft (DFG). The authors would like to thank A. Blume for preparing the crystals.

References

[1] J. Haber, in: *Handbook of Heterogeneous Catalysis*, vol. 4, ed. G. Ertl, H. Knözinger and J. Weitkamp (Wiley-VCH, Weinheim, 1997).
[2] F.J. Janssen, in: *Handbook of Heterogeneous Catalysis*, vol. 4, ed. G. Ertl, H. Knözinger and J. Weitkamp (Wiley-VCH, Weinheim, 1997).
[3] L. Fiermans and J. Vennik, Surf. Sci. 9 (1968) 187.
[4] E. Gillis, Compte Rend. Acad. Sci. Paris 258 (1964) 4765.
[5] J. Haber, M. Witko and R. Tokarz, Appl. Catal. A: General 157 (1997) 3.
[6] D.S. Su, M. Wieske, E. Beckmann, A. Blume, G. Mestl and R. Schlögl, Catal. Lett. 75 (2001) 81.
[7] D.S. Su and R. Schlögl, submitted to Catal. Lett.
[8] F. Zemlin, E. Beckmann and K.D. Vandermast, Ultramicroscopy 63 (1996) 227.
[9] H. Schäfer, *Chemische Transportreaktionen* (Verlag Chemie, 1962).
[10] R. Enjalbert and J. Galy, Acta Cryst. C: Cryst. Struct. Commun. 42 (1986) 1467.
[11] R. Egerton, *Electron Energy-Loss Spectroscopy in the Electron Microscope* (Plenum Press, New York, 1996).
[12] D.S. Su, V. Roddatis, M. Willinger, G. Weinberg, E. Kitzelmann, R. Schlögl and H. Knözinger, Catal. Lett. 74 (2001) 169.
[13] P.L. Gai, Topics Catal. 8 (1999) 97.